Design of an electrochemically assisted radiation sensor for alpha-spectrometry of actinides traces in water

Jacques Sanoit (de), Thuan Quang Tran, Sylvie Pierre, Michal Pomorski, Christine Mer-Calfati, Philippe Bergonzo

Design of an electrochemically assisted radiation sensor for α-spectrometry of actinides traces in water

Jacques de Sanoit[a,*], Thuan Quang Tran[a], Michal Pomorski[a], Sylvie Pierre[b], Christine Mer-Calfati[a], Philippe Bergonzo[a]

a CEA, LIST, Diamond Sensors Laboratory, F-91191 Gif-sur-Yvette, France

b CEA, LIST, Henri Becquerel National Laboratory, F-91191 Gif-sur-Yvette, France

* Corresponding author. Tel.: +33 1 69 08 86 75. E-mail address: jacques.desanoit@cea.fr

Abstract

We describe a new approach for the detection and identification of actinides at low activity levels directly in aqueous solution. The measurement consists initially, in immobilizing alpha emitters in the form of insoluble hydroxides onto the entrance window of an immersed alpha particles detector. For this, a boron doped diamond detector window is negatively polarized to produce a basic layer on its surface by water decomposition. Actinides elements that are known to be very sensitive to hydrolysis are precipitated as solid hydroxides onto the entrance window of the sensor. Due to the absence of an air layer between the radioactive source and the detector, there is no need for vacuum during the alpha spectrometry measurement. After analysis, the detector can be easily cleaned by anodization in the aqueous medium to be reused at once. The minimum detectable activity concentration (MDA) of the system has been evaluated with ^{241}Am at 0.5 Bq/L for a 0.33 cm^2 area Si PIN diode.

Keywords

Alpha spectrometry, Actinides, Electroprecipitation, Diamond electrode

1. Introduction

The quality of the water we use every day is an essential governing parameter of the public health. In our societies, the preservation of the integrity of the drinking water supply is considered as a major stake. The quality of this water can be affected more or less durably by numerous pollutants. Beside usual contaminants such as organic products (solvents…), heavy metals, and bacteriological pollutants, the quality of water can also be severely affected by radioactivity and should be controlled (European Commission, 2011). Radioactivity in water has mainly three origins. It can be either from natural, anthropogenic or could also result from hostile terrorist activity.

Among the multiple radionuclides, the actinide elements are of major importance due to their long half-lives of hundreds to hundred thousands of years, their radiation emission as well as their chemical toxicity to humans (Lizon and Fritsch, 1999). The light actinide elements, namely U, Np, Pu, Th, and Am, can exist in multiple oxidation states, (III–VI/or IV for Th and III–VII for Np), with each forming behaviorally distinct molecular species that can differ by orders of magnitude in reactivity, stability, and solubility (Vitorge, 1999). The range of potential reactions in natural aquifer systems is extremely broad because of the great variety of chemically active compounds in nature and the rich chemistry actinide elements exhibit (Choppin, 2003, Choppin, 2007). The conditions of the aquifer, such as pH, redox potential, complexing agent concentrations, and colloid concentration, determine the predominant

actinide species and their transport characteristics in the environment (Silva and Nitsche, 1995, Maher et al., 2013).

The analytical determination of actinide concentration levels in water by alpha spectrometry usually requires very long operations that involve the following sequence: (i) separation, (ii) purification, (iii) preparation of solid sources and (iv) counting and spectrometric detection (Holm and Fukai, 1977, de Regge and Boden, 1984, Bickel et al., 2000, Diakov et al., 2001, Ayranov et al., 2005, Salar Amoli and Barker, 2007). Under such operating conditions, the time required from sampling to the analytical result delivery extends over several days. Also, clearly the sample if evaporated can be considered as lost, thus it remains a test sample approach. In the proposed approach, the detection of actinides is much faster, the sample is not destroyed, thus this becomes a real breakthrough for the consumer.

We propose to realize a novel sensor enabling to probe the activity concentration of trace levels of actinide contaminants in water. To date, there is no system enabling evaluation of water activity using a portable, easy to handle system that can be established for early stage detection of nuclear accidents as well as for continuous water quality control. Primary target is fresh water control, but in the future the detection system could be also used for water reservoir monitoring, for waste water assessment, for soils as well as for drinking products.

Water immersed detectors for α activity monitoring in solutions containing traces of actinides ions have been addressed for a long time. In fact, as early as in 1977, natural diamond had already been successfully tested as detector material of α particles in concentrated plutonium solutions in nitric acid media (2 M) with concentrations ranging from 10 to 100 mg/L of ^{239}Pu (Kozlov et al., 1977). In this configuration the volume probed by the active surface of the device corresponds to the volume of liquid through which alpha particles can penetrate, thus it is limited to typically a few tens of micrometers. Although this technique allows getting round the delicate problem of the α-source preparation, it can only probe in real-time extremely high activity levels, and therefore is not suitable for monitoring traces in fresh water. Later in 2000, the detection technique was improved at CEA (French Atomic Energy Commission) by the use of synthetic diamond as active alpha-sensor which was deposited on silicon substrate using Plasma Enhance Chemical Vapor Deposition (PECVD). Prototypes were fabricated for monitoring alpha activity in acids and concentrated solutions in nuclear reprocessing plants (Bergonzo et al., 2000). Some of these devices are currently in use at the Rakkasho Mura reprocessing plant (Japan) under operation by Japan Nuclear Fuel Limited (JNFL). More recently, PIPS® detectors (Passivated Ion implant Planar Silicon—*a Canberra Silicon based technology for radiation detection*) have been used to detect α particles on the surface of a liquid (Egorov et al., 2005). Although these devices are not a part of the family of immersed detectors, the experimental purpose remains similar: direct detection conducted without any pre-enrichment and reduction of the corrosion degradation from the radionuclide acidic solution. In 2005, Addleman and co-workers proposed a chemically enhanced alpha-energy spectroscopy in liquids based on extraction of actinides at pH 2 by a thin polymer film composed of di-2-ethylhexylphosphoric acid (HDEHP) and PVC deposited on a silicon diode (Addleman et al., 2005). In spite of this clever approach and consistent data collected with ^{241}Am, the reversibility of the membrane seemed to be not achieved for all actinides in particular when extraction is not pH dependent (^{239}Pu). In this case, decontamination of the sensor by pH variation is not possible and the membrane should be stripped off and renewed

before being used again. Furthermore, no kinetics data on actinides extraction by the membrane sensor were given by the authors.

We will introduce another innovative approach that will be a real breakthrough for sensitive detection consisting of depositing actinides using an electrochemical technique directly onto a boron doped diamond entrance window of an alpha sensor acting as an electrochemical cathode. On the one hand, diamond is a low atomic number material convenient for detector window fabrication with respect to alpha lines attenuation. On the other hand, boron doped diamond is a very attractive material for electrochemists. It possesses several interesting properties and namely hardness, high resilience to corrosion and radiation damage in harsh environment (Bergonzo et al., 2003) combined with very particular electrochemical properties. Highly doped diamond exhibits a large potential window (3.2 V in aqueous solution), high electron transfer rate (k0>0.1 cm/s) with outer sphere redox couples combined with low backing currents (Vanhove et al., 2007, Vanhove et al., 2009). Boron is by far the most widely used doping agent to produce conducting p-type semi-conductor diamond (Thonke, 2003). This is because boron has a low charge carrier activation energy of 0.37 eV (Haenni et al., 2004). At high doping levels (>3×10^{20} boron atoms cm^{-3}) the material acts as a semimetal (Lagrange et al., 1998). If boron doped diamond electrodes are fouled in dirty environments (biological fluids…), they can be electrochemically re-activated by cyclic (de Sanoit and Van Hove, 2007), pulsed (Mahé et al., 2005), or pulsed in situ (Kiran et al., 2011, Kiran et al., 2013) electrochemical methods within several media. Thin electroactive films of synthetic boron doped nanocrystalline diamond (B-NCD) can be synthesized at rather low cost using a mixture of hydrogen/methane as carbon precursor and trimethylboron (TMB) as doping agent, at temperatures from 500 °C to 800 °C, by microwave assisted chemical vapor deposition (CVD) on silicon substrates.

It is known that the electrodeposition of actinides, i.e. their reduction at the metallic state with a charge transfer, is impossible with respect to the very negative standard potentials of these elements (Vitorge, 1999). However, in aqueous acid solution, the potential window is limited by the electrochemical water decomposition (on the reduction side through the system H_2/H^+ and on the oxidation side through the system H_2O/O_2). In addition, no electrochemical activity can be undertaken beside the electrochemical decomposition of the solvent. The whole current crossing the electrode being used for these reactions building what the electrochemists call the "solvent wall". One can overcome this experimental difficulty by taking into account that actinide ions are very sensitive to hydrolysis (Altmaier et al., 2013). By increasing the pH of an aqueous solution containing actinide ions, the structure of ions is modified: protons become expelled by water hydration molecules towards non-binding water, the actinide ions accumulate hydroxyl ions (OH−) in the internal sphere and form hydroxo mono or polynuclear complexes (Baes and Mesmer, 1986) with solid hydroxides as final products. As a result, ion hydrolysis of actinides will not take place as long as they are kept in acidic solutions with concentration above 1 M or/and by the addition of complexing ions which will delay the aforementioned hydrolysis reactions. It is easy to locally modify the pH near the surface of the working electrode by electrochemical water reduction, a reaction that results in the formation of a basic layer (pH 12–13) according to the following reaction:

$$H_2O + H^+ + 2e^- \rightarrow OH^- + H_2 \qquad (1)$$

For example, the electroprecipitation of insoluble trivalent actinide hydroxide onto the cathode can thus be carried out even in slightly acidic solution according to reaction

$$M^{3+} + 3OH^{-} \rightarrow M(OH)_3 \qquad (2)$$

More information on actinides insoluble hydroxide compounds versus oxidation states has been discussed by Vitorge in a review (Vitorge, 1999).

When the reduction current is switched off, the basic layer disappears and the actinide hydroxide can dissolve more or less quickly in the acid liquid medium. This can be avoided by adding ammonia into the electrolyte just before switching off the current. In the following, we introduce a method of electro-precipitation of actinide ions in aqueous media containing sodium sulfate or nitrate (or a mixed of both) as complexing agent. The sulfate method was initiated by Talvitie in (1972) then was modernized successively by Becceril-Vilchis in (1996) and by Tsoupko-Sitnikov in (2000). This alternative of the initial method developed by Talvitie was optimized to work at the same time on revolving and static cathodes. When compared to other works (Glover et al., 1998, Bajo and Eikenberg, 1999) or (Payne et al., 2001), the method proposed by Becceril-Vilchis and Tsoupko-Sitnikov uses only low current densities to obtain high deposition efficiencies for the actinide ions on stainless steel substrates. The current approach is based on electroprecipitation of actinides on diamond/silicon detector composite material. To realize the first prototypes, B-NCD was grown on two different substrates: (i) high resistive silicon or (ii) silicon PIN diode.

2. Experimental

2.1. Radioactive standards and chemicals

^{241}Am (main energy line; Eα=5.49 MeV), ^{239}Pu (Eα=5.16 MeV) and ^{244}Cm (Eα=5.80 MeV) stock solutions were supplied in [HNO_3]=1 M by LNHB (Henri Becquerel National Laboratory, France). Aliquots of these solutions were converted to the sulfate form by evaporating to dryness and dissolution of the dry residue into [H_2SO_4]=1 or 2 M (for plutonium). After these chemical adjustments, the radioactive solutions were measured by liquid scintillation counting using 10 mL Ultimagold AB (Packard) as scintillation cocktail in plastic flask, to become our final activity standards; ^{241}Am (238±2) Bq/ml, ^{244}Cm (176±2) Bq/ml and ^{239}Pu (205±2) Bq/ml. We used a Wallac Guardian 1414 liquid scintillation counter, an all purpose digital liquid scintillation counter based on digital spectrum analysis controlled under a Microsoft Windows platform. Analytic grade, sulfuric and nitric acids, ammonia, sodium sulfate, sodium nitrate, potassium ferrocyanide trihydrate, potassium ferricyanide and potassium chloride were supplied by Sigma Aldrich and used without any further purification. Deionized water (DI) used for aqueous solutions preparation was produced by a Direct Q3 water purification system (Millipore).

2.2. Sensors design

Two generations of sensors were produced for the purpose of measuring the actinides traces in liquid phases with the electrochemically assisted pre-concentration step. (i) The first generation sensors so-called counter grade (CG–B-NCD/Si structure) sensors allow counting of alpha particles emitted by decaying actinide atoms with clear separation of induced signals from electronic noise and alpha-particle detection efficiency close to 100% (2π geometry). (ii)

Improved second generation sensors so called spectroscopic grade (SG–BNCD/Si PIN), allow both actinides counting and identification through the alpha particles energy loss spectroscopy. For the (i) CG-BNCD/Si sensors fabrication, we used as substrates thin (200 µm) high resistivity (10^4 Ω cm) intrinsic silicon wafers, whereas in the case of (ii) spectroscopic-grade sensors commercial *Siemens* Si-PIN diodes were used. In a first step, the original diode metallization was stripped-off using a hot aqua-regia ($HCl:HNO_3$: 3/1) solution. The bare substrate was then rinsed with DI water and dried. In the second step, the p+ surface of the diode (or one surface of silicon wafer) was seeded with aqueous solution of diamond nanoparticules using a spin-coating method. Diamond nanoparticles were produced by the detonation technique and provided by the Nanocarbon Research Institute Co., Ltd (Japan). Such prepared samples are loaded into a microwave-plasma assisted chemical vapor deposition (CVD) reactor. We used Trimethylboron (TMB) as doping agent precursor to obtain highly boron doped (3×10^{21} boron atoms cm^{-3}) diamond films (Vanhove et al., 2009). One must note that the B-NCD electrode will correspond to the dead detector volume not participating in the signal formation, thus it must be kept as thin as possible, typically in the range of 150–450 nm, although pin-hole free films with thickness below 150 nm are also readily achievable. After diamond growth, the central area of about 0.8 cm^2 in our prototypes was masked using a 200 nm aluminum sputtered mask and in the following step, peripheral regions of B-NCD were etched using Ar/O plasma. Later, the aluminum mask was stripped-off in aqua-regia solution. The back surface of the diode (and high resistivity silicon) was coated with 200 nm of gold forming an ohmic back contact. The device was mounted onto an insulating holder and contacted with a coaxial cable using silver loaded epoxy resin. We used a highly resistive and electrochemically inactive bi-component epoxy resin (Bostik) to encapsulate the device leaving only a B-NCD diamond entrance electrode exhibiting a direct contact with the analyzed solution. The active B-NCD area was measured using an image of the diamond area taken with an optical microscopy facility and by integrating its surface using image processing software. Prior to the measurements in radioactive solutions, the properties of each B-NCD electrode were evaluated using standard electrochemical techniques such as cyclic voltametry and electrochemical impedance spectroscopy (at open circuit potential) in an equimolar solution of $K_3[Fe(CN)_6]/K_4[Fe(CN)_6]=10^{-3}$ M as outer-sphere redox couple and [KCl]=0.5 M as supporting electrolyte.

2.3. Actinides deposition kinetics

Reaction kinetics of actinides deposition on B-NCD is an important aspect of the electrochemical study. Kinetics data should be collected in order to adjust the minimum electrolysis time necessary for reaching the maximum deposition yield. For this, several B-NCD (450 nm)/boron doped Si (430 µm) substrates with resistivity <0.005 Ω cm were mounted down at the bottom of a conical shape 20 ml volume Plexiglas cell (Karlsruhe Institute of Technology, Germany) leading a bare 1.2 cm^2 surface diamond cathode (see Fig. 1a). The cell was filled by 18 ml of aqueous electrolyte spiked by aliquots of ^{241}Am, ^{239}Pu and ^{244}Cm standards at a same activity level (5.96, 5.13 and 4.40 Bq respectively). Electroprecipitation of actinides was performed in batch experiments after pH and complexing salt adjustment and under vigorous mechanical stirring (10^3 rpm) for deposition times ranging from 15 to 120 min. pH and complexing agent allow controlling hydrolysis reactions and the charge of salt provides good conductivity of the electrolyte reducing the voltage drop across the electrolytic cell. The electro-precipitation of actinide ions on the

surface of boron doped diamond was achieved by connecting a negative bias to the silicon layer of the B-NCD/Si composite and the positive one to a platinum wire anode. The chosen deposition parameters were (i) [Na_2SO_4]=0.3 M adjusted at pH 3.5 with H_2SO_4 and cathodic current density; J_c=−5 mA/cm^2 and (ii) [$NaNO_3$]=0.3 M adjusted at pH 3 with HNO_3 ; J_c=−2.5 mA/cm^2. In this last case (ii) initial pH and current density were chosen at lower values in comparison to (i) conditions because of the release of excess of OH^- due to nitrate reduction which would induce a too fast increase of the pH. Spectrometric data from the layers were collected with an external alpha spectrometry chain with well defined solid angle geometry from the LNHB facilities and described elsewhere (Pierre et al., 2010).

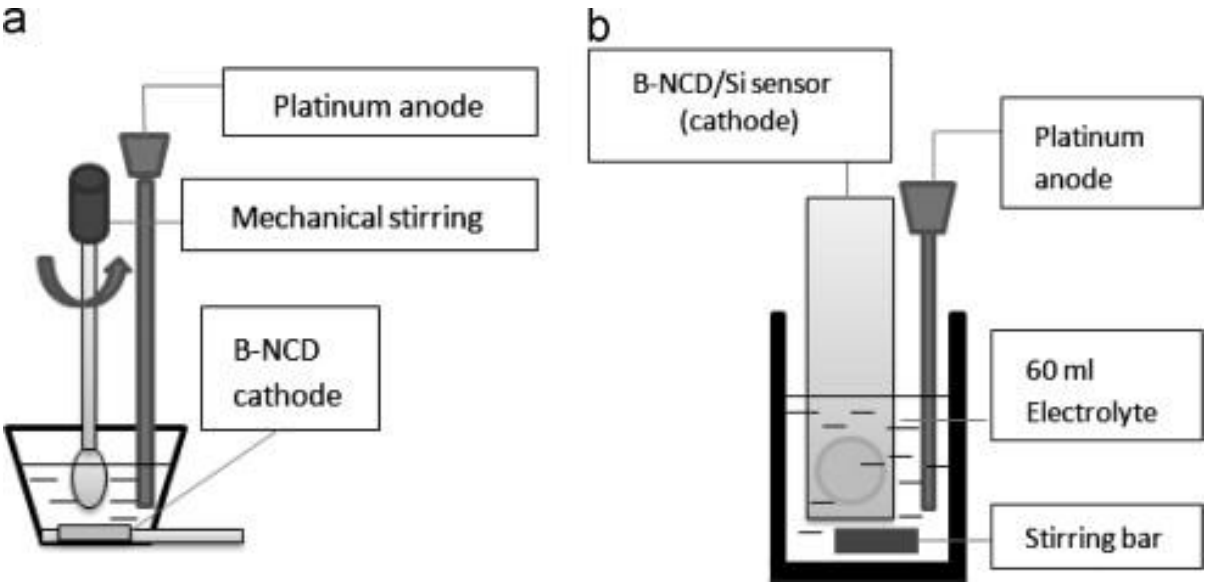

Fig. 1. Electrochemical cell geometries used (a) deposition kinetics studies. (b) Deposition on sensors. (a) Conical shape 20 mL cell and (b) Glass 100 ml Cell.

2.4. Deposition of actinides on sensors

Electroprecipitation of actinides on sensors were carried out using ^{241}Am alone (or a mixture with other actinides) as radioactive tracer(s) in a purpose-built two-electrodes one-compartment glass cells containing 15–80 ml of aqueous electrolyte. A platinum wire and the B-NCD sensor window (cathode) connected to a LKB Macrodrive 2301 electrophoresis power supply were respectively used as counter and working electrodes. The aqueous medium containing actinides was chemically adjusted in both pH and complexing salt concentration (Na_2SO_4, $NaNO_3$ or a mixture of both). Solution stirring (10^3 rpm) was done by mean of a Teflon-coated magnetic rod. The experimental arrangement is shown in Fig. 1b. The experimental conditions for all sensor data shown in the text are presented in Table 1.

Sensor type	Surface (cm^2)	Actinide	Activity (Bq)	$[Na_2SO_4]$ (M)	$[NaNO_3]$ (M)	Volume (mL)	pH	Deposition time (min)	Current density (mA/cm^2)	Stirring (r.p.min)
CG	0.40	^{241}Am	4.76	0.3	0	60	3	90	−5	10^3
CG	0.17	^{241}Am	0.6–28	0.3	0	40	4.5	120	−6	10^3
SG	0.33	^{241}Am	5.96	0–0.3	0–0.3	60	2.17–4.20	90	−5	10^3
SG	0.33	^{241}Am	6–36	0.3	0	80	3	120	−9	10^3
SG	0.40	^{239}Pu ^{244}Cm	n. a.	0.3	0	80	4	90	−6	10^3
SG	0.25	^{239}Pu ^{241}Am ^{244}Cm	5.13 5.96 4.40	0	0.3	15	3	90	−5	10^3
SG	0.40	^{239}Pu ^{244}Cm	9.98 10.02	0.3	0	60	3.9	120	−2.5	10^3

Table 1. Experimental conditions for electroprecipitation of actinides on SG–BNCD/Si and SG–BNCD/Si PIN sensors (CG: counting grade sensor; SG: spectroscopic grade sensor).

2.5. Alpha particles detection system

After electroprecipitation of actinides, the sensor was connected to an electronics spectroscopic chain as depicted in Fig. 2. A custom made Fast Charge Sensitive Amplifier (FCSA) was used to amplify and to shape the alpha-particle induced current signal, which was later digitized and registered on a digital-storage oscilloscope (DSO, Le Croy Waverunner). The alpha particles from the precipitated actinides layer on the diamond film will interact in the silicon ionization chamber inducing current pulses. The number of counts recorded by the detector is proportional to the amount of alpha emitters present at the diamond surface, and the signal amplitude to the characteristic alpha energy allowing actinides identification. As a result, it becomes very accurate to probe the actinides concentration and origin in the solution thanks to a prior device calibration with activity standards.

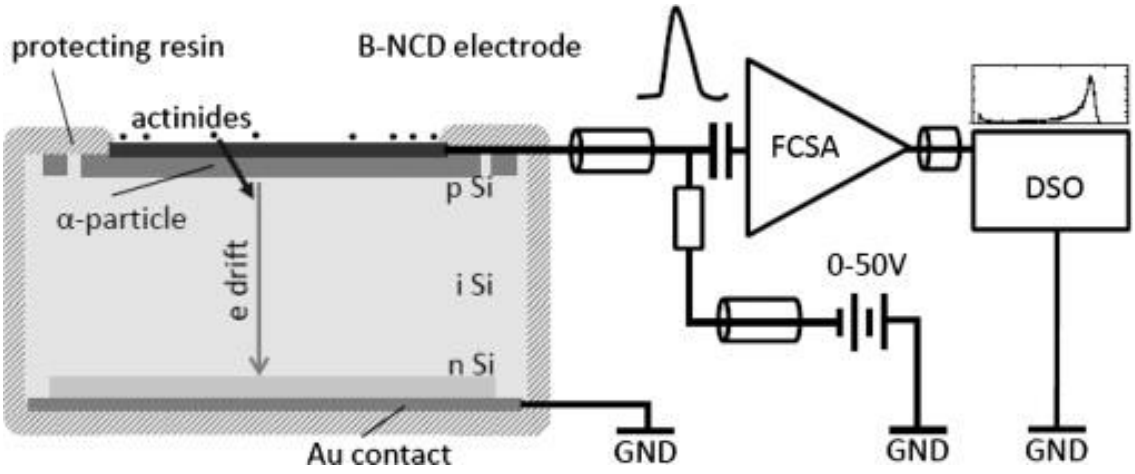

Fig. 2. Sensor experimental arrangement for alpha-particles detection.

2.6. Sensors cleaning

After alpha-spectrometry measurement, a light anodization of the sensors (+6 mA/cm^2 for 10 min in a new aqueous electrolyte) simply results in the release of most of the preconcentrated actinides species into the solution. This enables cleaning the active surface layer prior to the subsequent measurement. After each cleaning procedure, the residual activity on the sensor was checked by alpha spectrometry for several hours of counting. Standard decontamination yield value was found to be more than 99% in most cases.

3. Results and discussion

3.1. Deposition of actinides on B-NCD/Si

Kinetics data of actinides deposition on 1.2 cm^2 surface area B-NCD/Si substrates are presented in Fig. 3. On the one hand, maximum deposition yields around 80% are obtained in nitrate media for Am and Cm in comparison to 70% for the sulfate one. On the other hand, plutonium deposition seems to be less efficient with only 38 and 42% for the same deposition time. From this plot, deposition time of 90 min seems to be the minimum value to reach equilibrium for the electroprecipitation at the used conditions. Due to nitrate reduction by-products (see below Eqs. (6), (7), (8)) a regular pH increase of the nitrate electrolyte was observed (from 3.0 to 3.8) during the actinides deposition in contrast to the sulfate medium where the pH remains at a constant value.

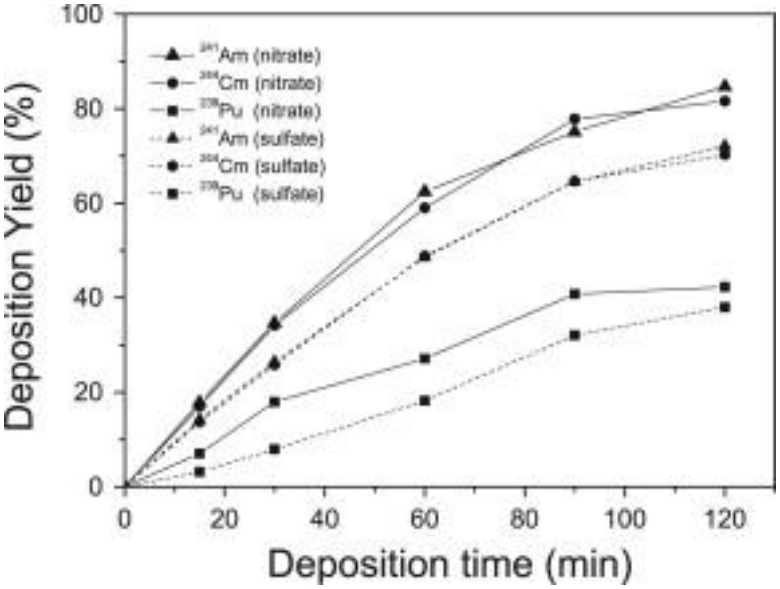

Fig. 3. Deposition kinetics of ^{241}Am (5.96 Bq), ^{239}Pu (5.13 Bq) and ^{244}Cm (4.40 Bq) on B-NCD/Si substrates, [Na_2SO_4]=0.3 M at pH 3.5 with J_c=−5 mA/cm^2, [$NaNO_3$]=0.3 M at pH 3 with J_c=−2.5 mA/cm^2, electrolyte: 18 ml, cathode surface area: 1.2 cm^2, and stirring rate: 10^3 rpm.

We studied the variation of the actinide deposition yield versus B-NCD/Si substrate surface area for two electrolytes compositions ([$NaNO_3$]=0.3 M, pH 3 and [$NaSO_4$]=0.3 M, pH 4) using ^{241}Am (5.96 Bq) as radioactive tracer. The other experimental conditions were J_c=−3 mA/cm^2, 90 min deposition time and 15 mL electrolyte volume. The deposition yield of ^{241}Am increase to 71% ($NaNO_3$) and to 49% (Na_2SO_4) with the cathode surface but without evidence any linear variation. The experimental results are shown in Fig.4.

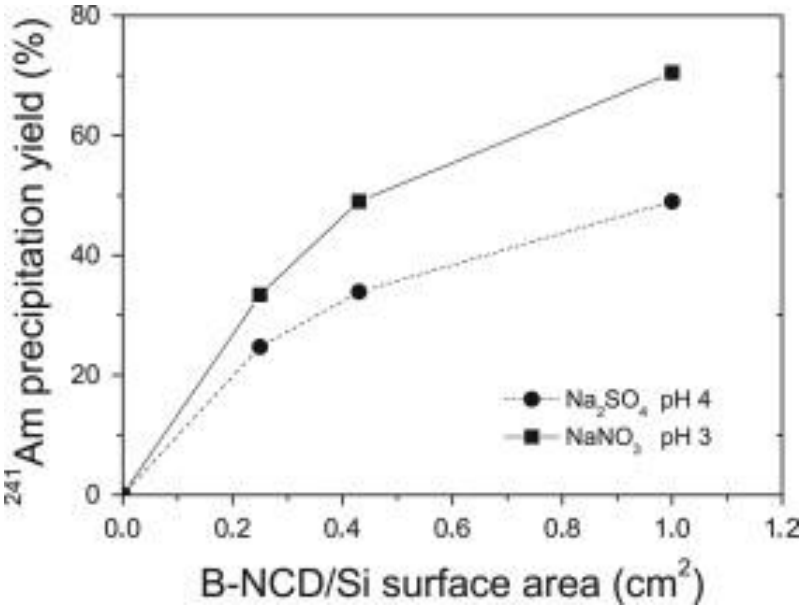

Fig. 4. Variation of the ^{241}Am deposition yield versus B-NCD/Si surface area ^{241}Am (5.96 Bq); electrolyte volume (15 mL), J_c=−5 mA/cm^2, stirring rate: 10^3 rpm [Na_2SO_4]=0.3 M at pH 4 and [$NaNO_3$]=0.3 M at pH 3.

3.2. Performance of CG-BNCD/Si sensors

To study the influence of the actinides layers on the sensor response (CG–BNCD/Si), we used at first a 4 kBq spectrometric grade ^{241}Am source (LEA-CERCA, France) deposited on a stainless steel substrate. The set radioactive source/sensor was put under primary vacuum before the spectrum was recorded. This configuration simulates the usual configuration used in alpha spectrometry. Secondly, we measured an ^{241}Am deposit on the sensor prepared according to our electrochemical process ([Na_2SO_4]=0.3 M at pH 3 and J_c=−5 mA/cm^2 for 90 min). In a third experiment, a drop (20 μL) of an ^{241}Am standard solution in sulfate medium is poured directly on the entrance window of the sensor (area=0.4 cm^2). After drying this deposit under air, the spectrum is recorded. The three corresponding plots normalized to maximum counts are shown in Fig. 5. As expected, the spectrum from the liquid source poured and dried on the sensor entrance window has a very poor spectroscopic quality. This can be explained by the presence of a solid sulfate salt residue that causes a high level of energy attenuation of the alpha particles producing a significant energy shift. Both other spectra are practically overlapped. This shows unmistakably that the qualities of both sources are comparable and consolidate our technological choice for the realization of the device.

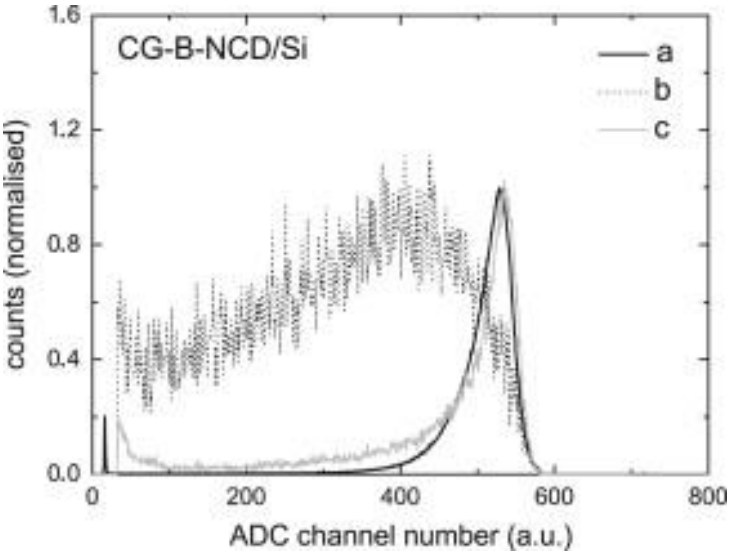

Fig. 5. Comparison of ^{241}Am spectra obtained with a CG–BNCD/Si sensor under different operating conditions. (a) Spectroscopic grade ^{241}Am source measured under vacuum, (b) radioactive drop poured and dried directly on the detector and (c) electroprecipited source in $[Na_2SO_4]$=0.3 M at pH 3 on the sensor.

The linear response of the CG–BNCD/Si sensor has been assessed using ^{241}Am aliquots as radioactive tracer. We plot the recorded counts/2π or the counting rate ($s^{-1}/2\pi$) after electroprecipitation versus the ^{241}Am activity level (Bq) present in the electrolyte before deposition. Experimental results are shown in Fig. 6. A linear response of the sensor (R^2=0.995) was observed in the activity range studied (from 0.6 Bq to 28 Bq).

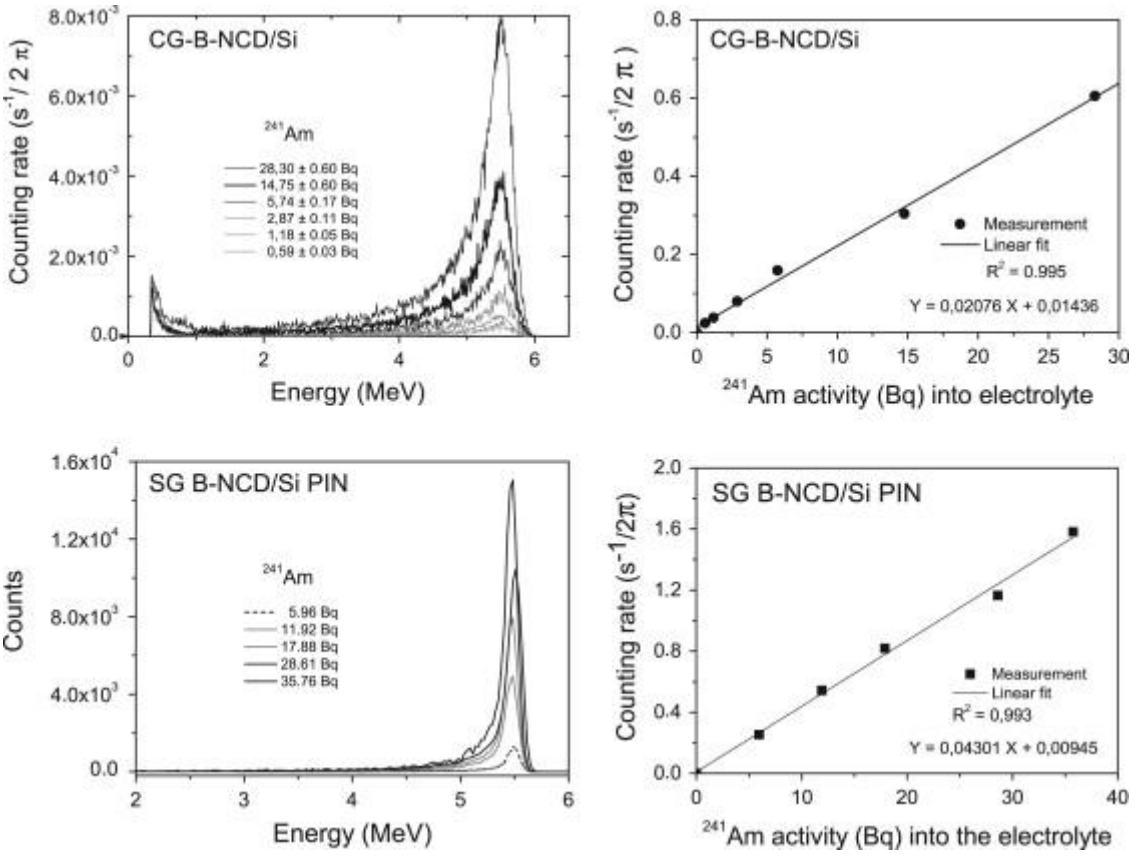

Fig. 6. Typical linearity data (counting rate vs activity) obtained with (i) A counting grade detector (CG–BNCD/Si), J_c=−6 mA/cm^2 for 2 h in 40 ml of [Na_2SO_4]=0.3 M adjusted at pH 4.5. (ii) A spectrometry grade detector (SG–BNCD/Si-PIN), J_c=−9 mA/cm^2 for 2 h in 80 ml of [$NaNO_3$]=0.3 M adjusted at pH 3.The stirring speed is 10^3 rpm for both.

3.3. Performance of SG-BNCD/Si PIN sensors

As a next step, a parametric study of electroprecipitation of actinides on a 0.33 cm^2 surface area SG–B-NCD/Si PIN sensor was done at constant current density (J_c=−5 mA/cm^2) for 90 min using ^{241}Am as radioactive tracer at 5.96 Bq/60 ml activity concentration level. The initial electrolyte pH was varied from 2 to 4 levels in Na_2SO_4, $NaNO_3$ and Na_2SO_4/$NaNO_3$ mixture. The experimental data are reported in Table 2.

Experiment	**[Na_2SO_4] (M)**	**[$NaNO_3$] (M)**	**pH electrolyte**	**pH variation**	**Counting rate (s^{-1}) *solution***	**Counting rate (s^{-1}) *dried***	**Deposition yield (%)**	**Cleaning yield (%)**
1	0.30	0	2.17	0	$(0.56\pm0.10)10^{-2}$	$(0.67\pm0.04)10^{-2}$	0.20±0.04	76.51
2	0.30	0	3.13	0	0.204±0.007	0.201±0.003	6.70±0.20	98.35
3	0.30	0	4.20	0	0.281±0.009	0.279±0.003	9.40±0.28	99.74
4	0.25	0.05	2.17	+0.05	$(0.85\pm0.13)10^{-2}$	$(0.97\pm0.05)10^{-2}$	0.30±0.06	85.68
5	0.25	0.05	3.17	+0.20	0.304±0.01	0.301±0.003	10.1±0.3	99.81
6	0.25	0.05	4.15	+0.85	0.210±0.01	0.244±0.003	8.20±0.25	99.51
7	0	0.30	3.07	+0.22	0.331±0.01	0.341±0.004	11.4±0.4	99.51

Table 2. Effect of electrolyte composition on electroprecipitation of actinides on SG–BNCD/Si PIN sensors Conditions: electrolyte; ^{241}Am 5.96 Bq/60 ml, J_c=−5 mA/cm^2 for 90 min with a stirring speed of 10^3 rpm, sensor: SG–B-NCD/Si PIN (area 0.33 cm^2).

During electrolysis in pure sulfate media (experiments 1–3 in Table 2), we observed no evolution of the pH value of the electrolyte. Thus this shows a perfect balance between the OH− generation at the cathode and protons at the platinum anode unless no reaction with sulfate ions which act here only as a non-electroactive supporting electrolyte. However, it is useful to specify that electrochemical oxidation of sulfate to peroxodisulfate (Serrano et al., 2002) (Provent et al., 2004) can take place in our device but only in the electrodecontamination mode where B-NCD is working as anode electrode. The reactions (see Eqs. (3), (4) below) that cannot be performed with “classical” electrode materials is due to the high value of the anodic potential at which the oxidation takes place (>+2V/NHE). In the present case, where the pH of the electrolyte is ranged between 3 and 4, the predominant species in the electrolyte is SO42− (pK1=−3, pK2=1.9 for H2SO4) so reaction (4) is the main reaction and the discharge of water (Eq. (5)) is a competition reaction

$$2\,HSO_4^- \rightarrow S_2O_8^{2-} + 2\,H^+ + 2\,e^- \qquad (3)$$

$$2\,SO_4^{2-} \rightarrow S_2O_8^{2-} + 2\,e^- \qquad (4)$$

$$H_2O \rightarrow \frac{1}{2}\ O_2 + 2\ H^+ + 2\ e^- \qquad (5)$$

In the presence of nitrate ions in the electrolyte (see experiments 4–7 in Table 2), nitrates ions can be reduced at the B-NCD cathode at a potential lower than −1.2 V/SCE (Levy-Clément et al., 2003) according to several concomitant reactions (see Eqs. (6), (7), (8)), all of them producing OH^- ions.

$$NO_3^- + H_2O + 2\ e^- \rightarrow NO_2^- + 2\ OH^- \qquad (6)$$

$$NO_3^- + 3\ H_2O + 5\ e^- \rightarrow N_2 + 6\ OH^- \qquad (7)$$

$$NO_3^- + 7\ H_2O + 8\ e^- \rightarrow NH_4OH + 9\ OH^- \qquad (8)$$

During nitrate reduction, due to OH^- ion formation, the pH of the electrolyte increases. Hydrogen evolution due to the reduction of water is the main parasitic reaction of nitrate reduction. It is also consisting of multi-steps reactions. The rate-limiting step in the sequence leading to hydrogen evolution also involves weakly adsorbed hydrogen intermediate. On boron doped diamond electrodes the hydrogen discharge occurs at lower potentials than for usual electrode materials (platinum, gold, glassy carbon…). This can be explained by adsorption of weakly bound hydrogen intermediates on the cathode.

After electro-precipitation of ^{241}Am on the sensor, two different ways for alpha-measurement were undertaken: (i) keeping the sensor immerged and (ii) drying the sensor after washing with deionized water. If we disregard results from experiments 1 and 4 where measurement uncertainties are very large (very weak deposition yields), data from Table 2 demonstrate that for a given experiment, both methods for counting the deposit (sensor in solution or sensor dried) gave a same recorded counting rate. This important observation thus allows us to glimpse the possibility of a measurement directly in the aqueous phase.

We observed that the precipitation yield of americium is very poor at pH 2 in Na_2SO_4 or in mixed $Na_2SO_4/NaNO_3$ electrolytes. The poor ^{241}Am recovery is linked to the high acid concentration of the electrolyte which disturbs the electrochemical generation of the hydroxyl layer on the B-NCD surface. We observed that the precipitation yield increases for the two kinds of electrolyte with the initial pH value due to the best efficiency for the hydroxyl layer generation. Nevertheless, a complementary experiment at pH 5 (not shown in Table 2) did not allow a deposition yield more than the maximum value obtained at pH 4.20 in sulfate medium. At this very low americium concentration level (5.96 Bq/60 ml–10−12 M Am), hydrolyzed species with subsequent polymerization and Am hydroxide will be formed in the electrolyte (Pershin and Sapozhnikova, 1990) and potentially adsorbed on the electrochemical cell walls. In contrast to Na_2SO_4 electrolyte, the maximum ^{241}Am precipitation yields (10%) in $Na_2SO_4/NaNO_3$ and 11% in $NaNO_3$ solutions were obtained at a lower pH (3.17 and 3.07 respectively). This can be explained by nitrate reduction reactions that produce large amounts of hydroxyl radicals as by-products (N_2, NH_4OH and NO_2^-) before water decomposition. These results show that optimized pH for the electroprecipitation of ^{241}Am in Na_2SO_4 and $NaNO_3$ buffer was 4.20 and 3.15 respectively. Electrodecontamination procedure shows a high efficiency greater than 99% in most cases. Lower decontamination factors were obtained with experiments 1 and 4 with the poorest precipitation yield.

The linear response of SG–BNCD/Si PIN has been assessed by the same method already described in Section 3.2.. Experimental results are shown in Fig. 6. A linear response of the sensors (R^2=0.993) was observed in the activity range studied (from 6 to 36 Bq).

The spectroscopy capabilities of SG-BNCD/Si PIN detectors were assessed using different mixed nuclides solutions of ^{239}Pu, ^{244}Cm and ^{241}Am. Measured mixed nuclides spectra probed after the electroprecipitation step are displayed on Fig. 7.

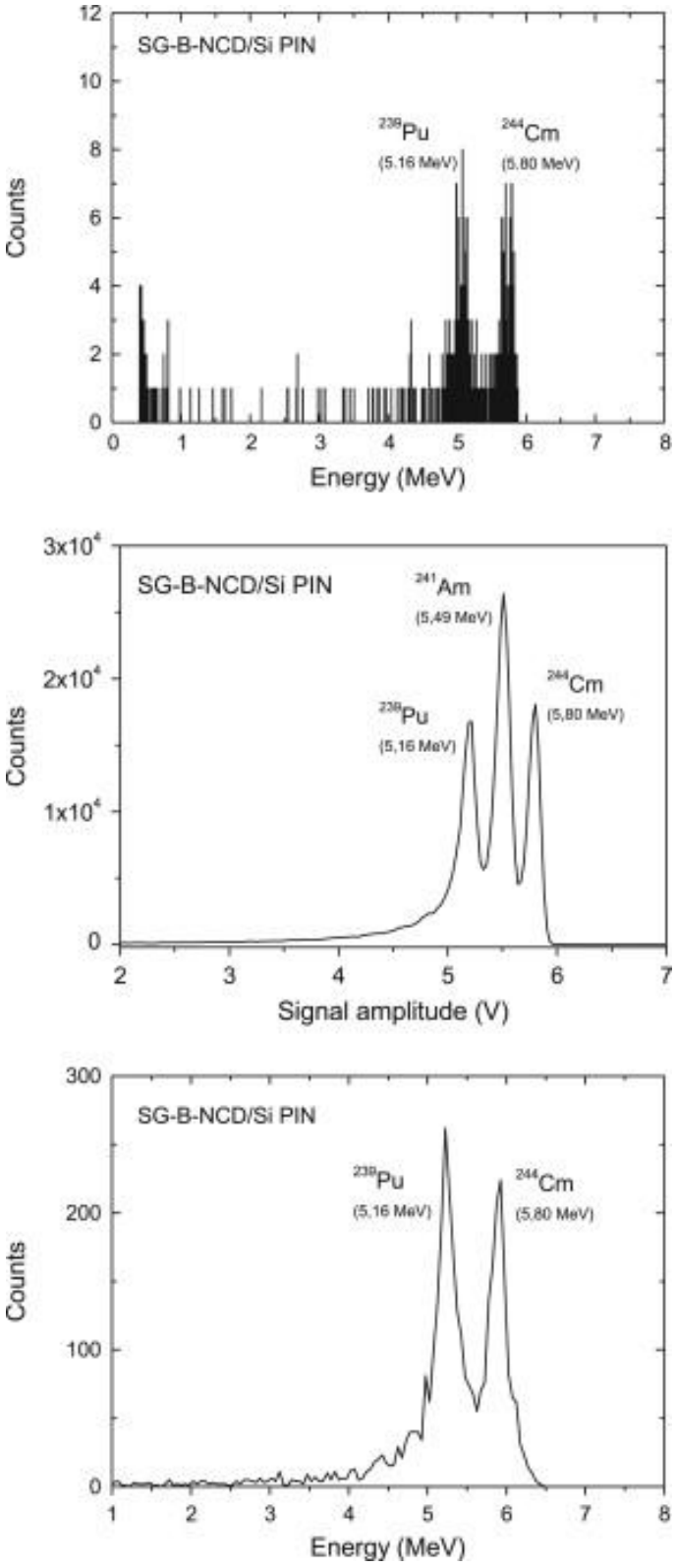

Fig. 7. Mixed nuclides spectra obtained with SG B-NCD/Si PIN sensors. (a) Alpha energy spectrum of an electroprecipited mixture of unknown activities of 239Pu and 244Cm coming from a very low level activity effluent operated at–20 V. Conditions: Jc -6 mA/cm2 in 80 ml of [Na2SO4] = 0.3 M at pH 4 for 90 min (sensor area 0.4 cm2). Identification has been done after 25 hours of counting (350 total counts). FWHM = 3.7 % for both actinides. (b)Alpha energy spectrum of an electroprecipited mixture of ^{241}Am (5.96 Bq), 239Pu (5.13 Bq) and ^{244}Cm (4.40 Bq) with Jc =–5 mA/cm2 in 15 ml of [$NaNO_3$] = 0.3 M at pH 3 for 90 min (sensor area = 0.25 cm2). FWHM = 3.3 % (^{239}Pu), 3.0 % (^{241}Am) et 2.3 % (^{244}Cm) and (c) Alpha energy spectrum of an electroprecipited mixture of ^{239}Pu (9.98 Bq), ^{244}Cm (10.02 Bq) with Jc =–2.5 mA/cm^2 in 60 ml of [Na_2SO_4] = 0.3 M at pH 3.9 for 120 min (sensor area = 0.4 cm^2) operated at – 20 V. FWHM = 4.4 % for both actinides

In the first example, the problem was to identify actinides with unknown and very low activity concentration level in an industrial effluent (distillate from an evaporation process). In this blind test, ^{239}Pu and ^{244}Cm were definitely detected (Full Width at Half Maximum (FWHM)=3.7%) after 90 min of electroprecipitation (J_c=−6 mA/cm^2, volume=80 ml, [Na_2SO_4]=0.3 M adjusted at pH 4 with H_2SO_4) with 350 counts (more or less 175 counts per radionuclide) recorded within 25 h.

The second example is a spectrum obtained after electroprecipitation of ^{239}Pu (5.13 Bq), ^{241}Am (5.96 Bq), and ^{244}Cm (4.40 Bq) for 90 min in a 15 ml electrolyte ([$NaNO_3$]=0.3 M at pH 3. In this case, the sensor is mounted down at the bottom of a one-compartment funnel shaped glass cell (nominal volume 25 ml) leading to a working area of 0.25 cm^2. A platinum wire is used as counter electrode and the aqueous electrolyte is stirred (10^3 rpm) with an agitator to a rotating electrode motor. The deposition yields were (19.1±0.6)% for ^{239}Pu, (36.7±1.1)% for ^{241}Am and (38.2±1.1) for ^{244}Cm. FWHM were found to be 3.3%, 3.0% and 2.3% respectively.

The third example is a spectrum recorded after electroprecipitation of 10 Bq each of ^{239}Pu and ^{244}Cm on a 0.4 cm^2 sensor for 120 min in 60 ml of [Na_2SO_4]=0.3 M at pH 3.9 for 120 min. The gross deposition yield was (11.2±0.4) %. FWHM were 4.4% for both actinides.

The three examples described here show that (i) identification of actinides is possible even at a very low activity concentration. The limiting factor becomes the counting time which has to stay in agreement with results delivery data delays. (ii) The present device allows reaching spectrometric resolution of several %. The use, in a near future of boron doped diamond layers grown on Passivated Implanted Silicon (PIPS) detectors should enhance the spectral resolution under the condition that the diamond growing process does not cause damage into the PIPS material (iii). Any other parameters (current density, stirring speed, electrolyte composition and cell geometry) being constant, the experiments results have shown that the increase of the deposition yield takes place by increasing the detector electroactive surface and by the decrease of the electrolyte volume.

3.4. Detection limit

Limit of detection (LOD) of our system is defined as the smallest quantity of actinides that will give a net signal above the system background. Currie (1968) proposed simple equations for LOD calculation which were until recently used. Today, due to the high performances of detection systems allowing reaching very low background noise, these equations are not

usable anymore. Another approach based on probability statistics in now used in alpha spectrometry (Ansoborlo et al., 2012). Because of the statistical fluctuations in the background noise, it is possible to detect a false peak that is a peak due to the background noise. This possible error is quantified by the risk which gives the probability α so that a radionuclide is detected while it is absent in the sample. Because of the statistical fluctuations in the signal, it is possible to detect a peak that is not real but rather due to the present activity in the sample and not due to the background noise. This possible error is quantified by the risk β which gives the probability that a radionuclide is not detected while being present in the sample. For α=β=5%, LOD can be expressed by expression

$$\mathrm{LOD} = 2.71 + 3.29\ (2\ B_n)^{1/2} \qquad (9)$$

where B_n is the mean value of several background measurements or value obtained in the case of a single measurement. Conversion to minimum detectable activity concentration (MDA) is given by expression

$$\mathrm{MDA} = k\ \mathrm{LOD} / (t\ R\ V) \qquad (10)$$

where k is the geometry factor (=2), t is the counting time for background determination (7200 s), R is the electroprecipitation yield and V is the volume (L) of the electrolyte.

For example, the SG–B-NCD/Si PIN sensor with 0.33 cm^2 surface area gives a background level in the ^{241}Am energy region of 4 counts per 120 min. Expression (10) allows, by taking into account various parameters as; LOD, deposition yield (10%), sample volume (60 mL) and detection geometry (2π), obtaining a MDA=0.5 Bq/L. This value appears acceptable since it remains in the range of activity of some of the highest radioactivity levels of some mineral waters (see e.g. Métivier and Roy, 1997).

3.5. Long term stability

Because such prototype detectors are meant to be reusable, several times after successive probing and cleaning steps, we have assessed the viability of large number of cleaning steps, and in particular if the successive anodization would risk causing damage to the diamond layer, or else to progressively alter e.g. the diamond grain boundaries. This was probed under visual analysis of the B-NCD surface under high magnification with a Field Emission Scanning Electron Microscope (Zeiss Supra 40). This study showed that after 72 cycles of anodization, no visible damage of the B-NCD layer was ever observed in comparison with reference samples not submitted to anodization (see Fig. 8). This result is in agreement with the work done by Duo et al. in (2004) that observed damage on B-NCD only for high current density (Ja=+1 A/cm2). Further work on the long term stability of a SG–BNCD/Si PIN sensor was done by recording (with a same acquisition time and without any modification of the spectrometer tuning), the first and last ^{241}Am spectra after thirty runs of electroprecipitation/decontamination. Peak height and energy resolution were kept constant and no form of shift could ever be observed on the alpha detection peak (see Fig. 9).

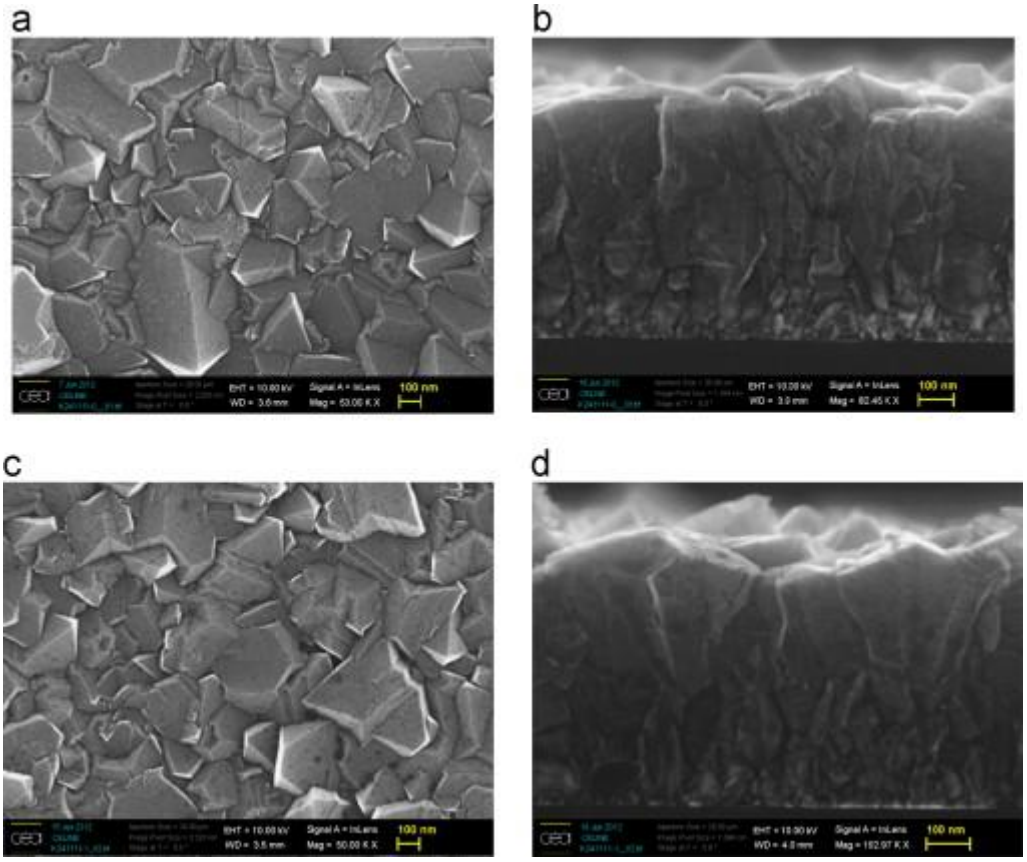

Fig. 8. SEM images of a 500 µm highly boron doped diamond layer grown on a silicon wafer (a and b) and the same sample after 72 runs of anodization (c and d) J_a=+6 mA/cm^2 for 10 min in [Na_2SO_4]=0.3 M adjusted at pH 4. (a) Top view of the B-NCD standard, (b) Cross section of the B-NCD standard, (c) Top view of the anodized sample and (d) Cross section of the anodized sample

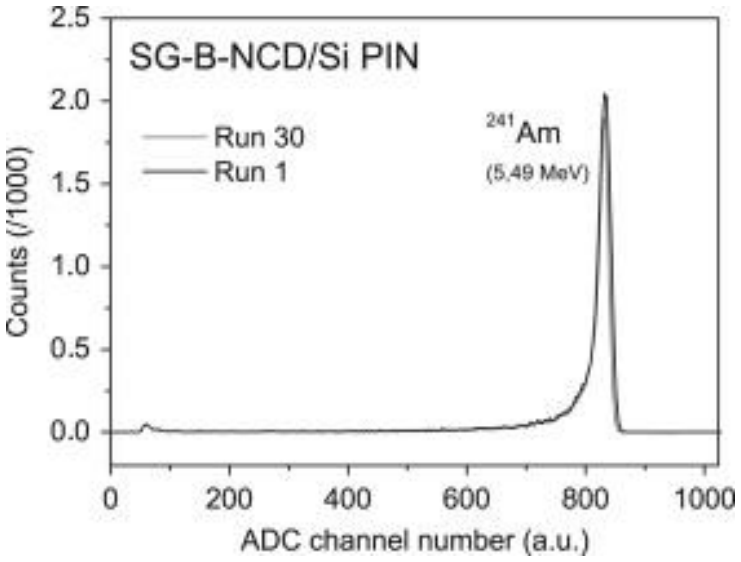

Fig. 9. Long term stability of a SG–BNCD/Si PIN sensor before and after 30 runs of deposition/decontamination deposition: J_c=−6 mA/cm^2 for 90 min/decontamination and J_a=+6 mA/cm^2 for 10 min in [Na_2SO_4]=0.3 M adjusted at pH 4.

3.6. Further work

Currently, the system remains under development and for example on-line measurement during electroprecipitation will be one of the next targets. Kinetics studies of electroprecipitation of actinides on B-NCD/Si substrates have shown that the deposition yield is enhanced by increasing the area of the electroactive surface. In a future work, it can be predicted that boron doped layers grown on large area PIPS detector (several cm^2 of surface area) will allow both improvement of spectrum resolution and precipitation efficiency. Another important aspect not addressed in this work is the influence of subsequent interfering hydrolysable cations such as iron, calcium (in spring water) or lanthanides (in nuclear effluent) which may tend to further reduce the efficiency due to competitive deposition process. On board microseparation strategies (e.g. lab-on a chip technology) are underway at the laboratory.

4. Conclusion

We have shown that it is possible to fabricate with synthetic diamond a device that is able to directly perform alpha-particle counting and alpha spectrometry in liquids using electrochemically assisted boron doped diamond/silicon sensors. The preconcentration step allows deposition of solid actinide hydroxides (^{241}Am, ^{239}Pu and ^{244}Cm tested) from nitrate or sulfate solutions directly onto the entrance B-NCD alpha detector window by low current density electroprecipitation. The obtained average precipitation yields for actinides in sensors designs remains low due essentially to the little surface area of the detectors used. This can be easily overcome using larger area sensors or via techniques enhancing of the actinide mass transport to the electrode from "Wall-Jet" geometry cells. This system consists of a jet of solution issuing from a circular nozzle which is allowed to impinge normally on a working disk electrode. Our work still demonstrated the ability to detect traces of actinides at levels as low as 0.5 Bq/L and identification in mixed low level alpha emitters solutions. Using a simple approximation, assuming a 5 cm^2 surface area of the CG-BNCD/Si PIN sensor and a mean value for electroprecipitation yield of 50% in a 40 mL volume sample during a 24 h counting duration, the detection limit for the current prototypes can be reduced to values as low as a few mBq/L. This technical approach has been patented (de Sanoit et al., 2011) and is now available for further development. The sensor decontamination technique can also lead to the fabrication of efficient electrochemical decontamination systems if large area B-NCD electrodes are used releasing the radioactive traces in dedicated waste water sample. Those devices can be therefore promoted to decontaminating systems when scaled up to several batches of several dm^2 surface area B-NCD electrodes. Such interest in boron doped diamond comes from its exceptional intrinsic properties including, a low *Z*, an extended electrochemical window, a very strong corrosion inertness enabling the device use in aggressive environments. Moreover, diamond synthesis is cost-effective since large area (2–6 in. in diameter) can easily be grown at reduce costs using chemical vapor deposition (CVD) technique.

Acknowledgments

Part of work presented here was supported by the ActFind Project, a Franco-German partnership on the global security granted by ANR (French National Agency for Research) and VDI Technologiezentrum GmbH. The authors would like to thank their German colleagues from the Fraunhofer Institutes (KIT and ICT) for valuable discussions during the course of this work. The authors express their sincere thanks to Philippe Cassette (Henri Becquerel National Laboratory, France) for technical assistance in liquid scintillation counting and Céline Gesset for SEM imaging.

References

R.S. Addleman, M.J. O'Hara, J.W. Grate, O.B. Egorov. Chemically enhanced alpha-energy spectroscopy in liquids. Radioanal. Nucl. Chem., 263 (2) (2005), pp. 291-294

M. Altmaier, X. Gaona, T. Fanghänel. Recent advances in aqueous actinide chemistry and thermodynamics. Chem. Rev., 113 (2013), pp. 901-943

E. Ansoborlo, J. Aupiais, N. Baglan. Mesure du Rayonnement Alpha, Editions TEC & DOC. Lavoisier, Paris (2012)

M. Ayranov, U. Krähenbühl, H. Sahli, S. Röllin, M. Burger. Radiochemical separation of actinides from environmental samples for determination with DF-ICP-MS and alpha spectrometry. Radiochim. Acta, 93 (2005), pp. 249-257

C.F. Baes, R.E. Mesmer. The Hydrolysis of Cations. (second ed.), Wiley, New York (1986), pp. 169-191

S. Bajo, J. Eikenberg. Electrodeposition of actinides for alpha-spectrometry. Radioanal. Nucl. Chem., 242 (3) (1999), pp. 745-751

A. Becerril-Vilchis, A. Cortès, F. Dayras, J. de Sanoit. A method for the preparation of very thin and uniform alpha-radioactive sources. Nucl. Instrum. Methods A, 369 (1996), pp. 613-616

P. Bergonzo, F. Foulon, A. Brambilla, D. Tromson, C. Jany, S. Haan. Corrosion hard CVD diamond alpha particle detectors for nuclear liquid source monitoring. Diamond Relat. Mater., 9 (2000), pp. 1003-1007

P. Bergonzo, D. Tromson, C. Mer. Radiation detection devices made from CVD diamond. Semicond. Sci. Technol., 18 (3) (2003), p. S105

M. Bickel, L. Holmes, C. Janzon, G. Koulouris, R. Pilvio, B. Slowikowski, C. Hill. Radiochemistry: inconvenient but indispensable. Appl. Radiat. Isot., 53 (2000), pp. 5-11

G.R. Choppin. Actinide speciation in the environment. Radiochim. Acta, 91 (2003), pp. 645-649

G.R. Choppin. Actinide speciation in the environment. J. Radioanal. Nucl. Chem., 273 (3) (2007), pp. 695-703

L.A. Currie. Limits for qualitative detection and quantitative determination. Anal. Chem., 43 (1968), pp. 586-592

A.A. Diakov, T.N. Perekhozheva, E.I. Zlokazova. Methods of high-sensitive analysis of actinides in liquid radioactive waste. Radiat. Measurements, 34 (2001), pp. 463-466

I. Duo, C. Levy-Clément, A. Fujishima, C. Comninellis. Electron transfer kinetics on boron-doped diamond Part I: influence of the anodic treatment. J. Appl. Electrochem., 34 (2004), pp. 935-943

O.B. Egorov, R.S. Addleman, M.J. O'Hara, T. Marks, J.W. Grate. Direct measurement of alpha emitters in liquids using passivated ion implanted planar silicon (PIPS) diode detectors. Nucl. Instrum. Methods A, 537 (2005), pp. 600-609

European Commission, 2011. Proposal for a council directive laying down requirements for the protection of the health of the general public with regard to radioactive substances in water intended for human consumption.

S.E. Glover, R.H. Filby, S.B. Clark, S.P. Grytdal. Optimization and characterization of a sulfate based electrodeposition method for alpha-spectrometry of actinide elements using chemometric analysis. J. Radioanal. Nucl. Chem., 234 (1) (1998), pp. 213-218

W. Haenni, P. Rychen, M. Fryda, C. Comninellis. Thin-film diamond part B. C. Nebel (Ed.), Semiconductors and Semimetals series, Academic Press (2004), p. 149 Elsevier

E. Holm, R. Fukai. Method for multi-element alpha-spectrometry of actinides and its application to environmental radioactivity studies. Talanta, 24 (11) (1977), pp. 659-664

R. Kiran, J. de Sanoit, E. Scorsone. Activation Process of a Diamond Electrode (2011). (Patent application no. 11 51341)

R. Kiran, E. Scorsone, J. de Sanoit, J.C. Arnault, P. Mailley, P. Bergonzo. Boron doped diamond electrodes for direct measurement in biological fluids: an in-situ regeneration approach. J. Electrochem. Soc., 160 (1) (2013), pp. H67-H73

S.F. Kozlov, E.A. Konorova, M.I. Krapivin, V.A. Nadein, V.G. Yudina, P.N. Lebedev. Usage of diamond detectors as immersed alpha-counters. IEEE Trans. Nucl. Sci., NS-24 (1) (1977), pp. 242-243

J.P. Lagrange, A. Deneuville, E. Gheeraert. Activation energy in low compensated homoepitaxial boron-doped diamond films. Diamond Relat. Mater., 7 (1998), pp. 1390-1393

C. Lévy-Clément, N.A. Ndao, A. Katty, M. Bernard, A. Deneuville, C. Comminellis, A. Fujishima. Boron doped diamond electrodes for nitrate elimination in concentrated wastewater. Diamond Relat. Mater., 12 (2003), pp. 606-612

C. Lizon, P. Fritsch. Chemical toxicity of some actinides and lanthanides towards alveolar macrophages: an in vitro study. Int. J. Radiat. Biol., 75 (11) (1999), pp. 1459-1471

E. Mahé, D. Devilliers, C. Comninellis. Electrochemical reactivity at graphitic micro-domains on polycrystalline boron doped diamond thin-films electrodes. Electrochim. Acta, 50 (2013), pp. 2263-2277

K. Maher, J.R. Bargar, G.E. Brown Jr. Environmental speciation of actinides. Inorg. Chem, 55 (2005), pp. 3510-3532

H. Métivier, M. Roy. Dose efficace liée à la consommation d'eau minérale naturelle par l'adulte et le nourrisson. Radioprotection, 32 (4) (1997), pp. 491-499

J.F. Payne, S.P. LaMont, R.H. Filby, S.E. Glover. Optimization and characterization of a sulfate based electrodeposition method for alpha-spectrometry of neptunium and curium. J. Radioanal. Nucl. Chem., 248 (2) (2001), pp. 449-452

A.S. Pershin, T.V. Sapozhnikova. Hydrolysis of americium (III). J. Radioanal. Nucl. Chem., 143 (2) (1990), pp. 455-462

S. Pierre, P. Cassette, M. Loidl, T. Branger, D. Lacour, I. Le Garrérès, S. Morelli. On the variation of the ^{210}Po half-life at low temperature. Appl. Radiat. Isot., 68 (7–8) (2010), pp. 1467-1470

C. Provent, W. Haenni, E. Santoli, P. Rychen. Boron-doped diamond electrodes and microelectrode-arrays for the measurement of sulfate and peroxodisulfate. Electrochim. Acta, 49 (2004), pp. 3737-3744

P. de Regge, R. Boden. Review of chemical separation techniques applicable to alpha spectrometric measurements. Nucl. Instrum. Methods, 223 (2–3) (1984), pp. 181-187

H. Salar Amoli, J. Barker. Rapid analysis of americium and plutonium in environmental samples by alpha-spectrometry. Indian J. Chem., 46A (2007), pp. 1618-1620

J. de Sanoit, M. Pomorski, C. Mer. Detection Method Using an Electrochemically-Assisted Alpha Detector for Nuclear Measurement in a Liquid (2011). (International Patent application number PCT/EP2011/067582)

J. de Sanoit, E. Van Hove. Procédé d'activation d'une électrode à base de Diamant, électrode Ainsi Obtenue et ses Utilisations (2007). (Patent application no. 0755485)

K. Serrano, P.A. Michaud, C. Comninellis, A. Savall. Electrochemical preparation of peroxodisulfuric acid using boron doped diamond thin film electrodes. Electrochim. Acta, 48 (2002), pp. 431-436

R.J. Silva, H. Nitsche. Actinide environmental chemistry. Radiochim. Acta, 70/71 (1995), pp. 377-396

N.A. Talvitie. Electrodeposition of actinides for alpha spectrometric determination. Anal. Chem., 44 (2) (1972), pp. 280-283

K. Thonke. The boron acceptor in diamond. Semicond. Sci. Technol., 18 (2003), pp. 520-526

V. Tsoupko-Sitnikov, F. Dayras, J. de Sanoit, D. Fillossofov. Application of rotating disk electrode technique for the preparation of Np, Pu and Am alpha-sources. Appl. Radiat. Isot., 52 (2000), pp. 357-364

E. Vanhove, J. de Sanoit, J.C. Arnault, S. Saada, C. Mer, P. Mailley, P. Bergonzo, M. Nesladek. Stability of H-terminated BDD electrodes: an insight into the influence of the surface preparation. Phys. Status Solidi A, 204 (9) (2007), pp. 2931-2939

E. Vanhove, J. de Sanoit, P. Mailley, M.A. Pinault, F. Jomard, P. Bergonzo. High reactivity and stability of diamond electrodes: the influence of the B-doping concentration. Phys. Status Solidi A, 206 (9) (2009), pp. 2063-2069

Vitorge. P., 1999. Chimie des actinides. Techniques de l'ingénieur. BN 3520 and Form. BN 3 520